25 July 1997, Revised 4 February 1998

ITEP-PH-5/97, CPPM/97-3, INP-MSU 97-18/469

On the search for muonic photons in neutrino experiments

V.A. Ilyin[1) *], L.B. Okun[2) †], A.N. Rozanov[3)‡]

* *Institute of Nuclear Physics, Moscow State University, Moscow 119899, Russia*
† *Institute of Theoretical and Experimental Physics, Moscow 117218, Russia*
‡ *CPPM, IN2P3-CNRS, Marseille, France*

(submitted to Nuclear Physics B)

Abstract

Conserved muonic number may turn out to be a conserved muonic charge, coupled to muonic photons, γ_μ. Muons and muonic neutrinos would emit γ_μ's, which might be discovered by analysing the data from the past and future high energy neutrino experiments (like CHARM II, CCFR, CHORUS [1], NOMAD [2], etc.). There are two sources of γ_μ's in these experiments: 1) internal bremsstrahlung in pion and kaon decays into μ and ν_μ, which provide neutrino beams; 2) external bremsstrahlung of muons in the shielding of the neutrino beam. In both cases the γ_μ's would pass freely through the shielding and produce narrow muonic pairs in the neutrino detectors. These pairs could be distinguished from the trident events $(\nu_\mu + Z \to \nu_\mu + \mu^+ + \mu^- + Z)$ by their kinematical properties: small p_t of the muon pair, small invariant mass, etc. All the above processes are quantitatively analysed in this paper.

PACS: 12.90+b; 13.15+g; 14.70Pw; 14.80.-j

Keywords: Muonic photons; Internal bremsstrahlung; External bremsstrahlung; Conversion to muon pairs; Tridents

1 Introduction

Speculations on the existence of massless vector particles (extra photons) coupled to baryonic number [3] and leptonic numbers [4]-[9] have been under discussion for several decades. In particular, three types of such photons – electronic, γ_e, muonic, γ_μ, and tauonic, γ_τ, – have been considered recently in ref. [5, 9] where the search for muonic photons at high energy neutrino experiments was discussed. In the present paper we undertake quantitative analysis of such a search by considering both the emission and the detection of γ_μ's.

As it is well known, the beams of muonic neutrinos in high energy neutrino experiments are formed in a long decay tunnel, where pions and kaons decay :

$$\pi^+ \to \mu^+ + \nu_\mu \ , \ \ \pi^- \to \mu^- + \bar{\nu}_\mu \tag{1}$$

$$\mathrm{K}^+ \to \mu^+ + \nu_\mu \ , \ \ \mathrm{K}^- \to \mu^- + \bar{\nu}_\mu \tag{2}$$

($\mathrm{K}_{\mu 3}$ decays are less important). The decay tunnel is followed by a thick shielding of iron, earth and concrete, which absorbs the beam of muons and all other secondary particles (hadrons and photons). For instance, in the neutrino beam of the CERN SPS the 185 meters of iron were followed by 173 m of earth, and again by 20m of iron and 15m of concrete [10]. The beam of muonic neutrinos passes through the shielding and produces reactions in the neutrino detector: mainly inelastic scattering on nuclei due to charged and neutral current interactions.

The idea of the search for muonic photons in neutrino experiments is based on the fact that the coupling constant of the muonic photons α_μ is small compared to $\alpha = 1/137$:

$$\alpha_\mu/\alpha < 10^{-5} \ . \tag{3}$$

This limit follows [4, 9] from the precision measurements of the $(g-2)_\mu$ – anomalous magnetic moment of the muon [11]. Because of smallness of α_μ, muonic photons would easily penetrate the shielding in the neutrino experiments and produce narrow muon pairs in the detector due to the reaction of the muon pair production by γ_μ in the Coulomb field of a nucleus with charge Z:

$$\gamma_\mu + Z \to \mu^+ + \mu^- \ + Z. \tag{4}$$

1) ilyin@theory.npi.msu.su
2) okun@vxitep.itep.ru
3) rozanov@cppm.in2p3.fr

On the other hand, the rates of emission of muonic photons and of production of muon pairs by them would be also small, which does not promise an easy hunt.

The main background for the process (4) are the so-called tridents:

$$\nu_\mu + Z \to \nu_\mu + \mu^+ + \mu^- + Z \ . \tag{5}$$

As we will show, the dimuon invariant mass distribution for tridents is broader, and these dimuons have much larger p_t-imbalance than in process (4), which may help to cope with the trident background.

To get accurate numerical results for the processes discussed in this paper we used the package CompHEP [12] to obtain analytical expressions for squared Feynman diagrams. For these purposes a new Lagrangian have been implemented to include new particle, muonic photon, and its interaction with muon and muonic neutrino. Then, for each process under the calculation, the FORTRAN code was generated for squared matrix element using the corresponding CompHEP option, as well as the phase space factor with proper regularization of kinematical singularities (see [13] for the description of regularization). The nuclear form-factors were implemented in this code as additional factors multiplying the matrix elements of reactions (4) and (5). The convolution with the spectra of muonic photons, muons or neutrinos was realized using the so called 'structure function' option of the CompHEP package. The phase space integration was performed with Monte-Carlo integrator BASES, while events were generated by the program SPRING, both programs are combined in the package BASES/SPRING [14]. The statistical error in our MC calculations was less than 1%. The results of CompHEP calculations are compared with the results of special CERN Monte-Carlo program in section 6 of this paper.

In this paper we present the theoretical basis for the search for muonic photons in a generic high energy neutrino experiment. The actual analysis of experimental data is possible only for collaborations, which run the experiments.

2 Emission of γ_μ's in pion and kaon decays.

The calculation of the internal bremsstrahlung in process (1) is straightforward, but the resulting spectrum has a simple analytical form only if one neglects the kinetic energy of the muon compared to $(m_\pi - m_\mu)$. Then for a pion decaying at rest we get:

$$\begin{aligned} dB(\pi \to \mu + \nu_\mu + \gamma_\mu) &\equiv \frac{d\Gamma(\pi \to \mu + \nu_\mu + \gamma_\mu)}{\Gamma(\pi \to \mu\nu)} = \\ &= \frac{2\alpha_\mu}{\pi} \cdot \frac{dx}{x} \cdot \left[(1 - x + \frac{1}{2}x^2) \cdot \ln \frac{2(1-x)}{m_{\nu_\mu}/(m_\pi - m_\mu)} - 1 + x \right] , \end{aligned} \tag{6}$$

where $x = \omega/\omega_{max}$, ω is the energy of the muonic photon and $\omega_{max} = (m_\pi^2 - m_\mu^2)/2m_\pi \approx m_\pi - m_\mu$. Expression (6) is infrared divergent, but this divergence has no adverse physical implications, because muonic photons of vanishing energy cannot produce muonic pairs. Another important feature of the expression (6) is its logarithmic dependence on the mass of the muonic neutrino. [4] This logarithm is due to configurations in which the photon and neutrino momenta are collinear. Thus, if one is lucky, one can not only discover the muonic photon, but to measure the mass of the muonic neutrino, even if it is extremely tiny and otherwise inaccessible. Both above features (infrared and collinear) are characteristic for the spectrum of internal bremsstrahlung in a general case, when the kinetic energy of muon is taken into account. To obtain accurate numerical results for the differential branching, in particular in the case of K decay, we evaluated analytically the squared matrix element with the help of the package CompHEP [12]. Then, the integration over squared invariant mass of neutrino and γ_μ was done analytically using the computer algebra system REDUCE [15]. The obtained expression was evaluated numerically with high accuracy by the corresponding REDUCE option. The results of these accurate numerical calculations, differ from (6) by a few percent in the case of pion. For the pion and kaon decays they are presented in table 1 for a set of neutrino masses, assuming $\alpha_\mu = 10^{-5}\alpha$. As can be seen on Table 1, diminishing the neutrino mass from 100 KeV to 10^{-10} eV increases the branching of the radiative pion decay only by a factor 7. If we would further decrease the neutrino mass to 10^{-100} eV that would further increase the branching only by a factor 10. It is hard to imagine the neutrino mass smaller than this scale. Note that the dimension of the visible universe is 10^{28} cm. The neutrino with such Compton wave length would have mass 10^{-33} eV.

A muonic photon with energy ω in the rest frame of a meson (pion or kaon) and angle θ (in the same frame) with respect to the direction of the meson beam has in the laboratory frame energy E_{γ_μ}, where

$$E_{\gamma_\mu} = \omega\gamma(1 + v\cos\theta) \ . \tag{7}$$

[4] This model assumes non-zero neutrino mass. But it can be so small, that no observable effects will be seen from neutrino mass, except for the radiation of muonic photons. The mass of the neutrino itself in this model gives the cut-off of the logarithmic divergence. It is well known that the theory of massless charged particles is infrared divergent. We consider small, but finite mass. Note also that the infrared problem in our case is much milder, than in QED of an almost massless electron, because our α_l is much smaller than the ordinary α. As a result the higher order corrections never become important.

Decay mode	$x = \omega/\omega_{max}$	$m_{\nu_\mu} = 100$ KeV	$m_{\nu_\mu} = 1$ eV	$m_{\nu_\mu} = 10^{-10}$ eV
$\pi \to \mu\nu_\mu\gamma_\mu$	0.9	0.367	1.37	3.39
	0.7	0.599	2.00	4.80
	0.5	1.01	3.25	7.74
	0.3	2.08	6.54	15.5
	0.2	3.50	10.9	25.6
	0.1	7.86	24.1	56.6
K$\to \mu\nu_\mu\gamma_\mu$	0.9	0.083	0.211	0.465
	0.7	0.127	0.304	0.657
	0.5	0.210	0.494	1.06
	0.4	0.289	0.675	1.45
	0.3	0.426	0.991	2.12
	0.2	0.712	1.64	3.51
	0.1	1.59	3.65	7.76
	0.07	2.35	5.37	11.4
	0.05	3.36	7.68	16.3
	0.04	4.25	9.70	20.6

Table 1: Internal bremsstrahlung: differential branching $dB/d\omega$ (in units of $10^{-5}\mathrm{GeV}^{-1}$, assuming $\alpha_\mu/\alpha = 10^{-5}$) as a function of the muonic photon energy, ω, for three different values of the muon neutrino mass, m_{ν_μ}, in the rest frame of decaying meson. The maximum photon energy is $\omega_{max} = (m^2_{\pi/\mathrm{K}} - m^2_\mu)/2m_{\pi/\mathrm{K}}$.

Here v is the velocity of the meson and $\gamma = 1/\sqrt{1-v^2}$. The spectrum of muonic photons is derived by integrating over $d\cos\theta$ and convoluting with the spectra of decayed pions and kaons. Photons are emitted within a cone with an angle $\theta' \sim 1/\gamma$. Thus, one should take into account the angular acceptance of the detector determined by the geometry of experiment (the length of the decay tunnel and the position and cross dimension of the detector). In this paper we use as an example the CHARM II neutrino detector at the 450 GeV CERN SPS neutrino beam. This detector is located at 882 m from the π/K production target with the length of the decay tunnel of 414 m. The formation of the γ_μ spectrum is discussed in [16] in details in the framework of a simplified approach to the simulation of the detector geometry and meson beam. As an example, we used the meson spectra from ref. [10] with the effective K/π-ratio equal 0.24. [5)]

The resulting spectra of muonic photons, produced by the internal bremsstrahlung, are presented in fig. 1.

An important feature of fig. 1 is that hard muonic photons are mostly produced in the kaon decays. Of course, it depends on geometrical parameters of the experiment (see [16]). However this feature could be taken into account in future experiments to increase possible yield of muonic photons produced by the internal bremsstrahlung.

In order to see the dependence of rates and spectra on the mass of the muon neutrino we present in fig. 2 the spectra of muonic photons for two values of the neutrino mass: $m_{\nu_\mu} = 100$ KeV - close to the experimental limit [11], and another assumed to be very small, $m_{\nu_\mu} = 10^{-10}$ eV. The yield of muonic photons is about seven times higher for the second choice of m_{ν_μ}. This allows one to hope that the mass of muonic neutrino could be measured in the experiments discussed, if muonic photon is discovered.

3 Emission of γ_μ's by muons in the shielding.

The effective material for the muon bremsstrahlung in the shielding is iron:

$$\mu + \mathrm{Fe} \to \mu + \gamma_\mu + \mathrm{Fe}. \tag{8}$$

The cross-section of the bremsstrahlung for the electron has been calculated by Bethe and Heitler [17, 18]; its derivation may be found in many text-books, e.g. [19, 20]. In the case of muon there is an obvious substitution $m_e \to m_\mu$. Moreover, the nuclear form-factor must be accounted for. This has been done by a group at the Moscow Engineering Physics Institute (MEPhI) [21]-[24], see also [25]-[27]. In order to apply their expressions to the process (8) we have to multiply them by α_μ/α. In the ultra-relativistic limit, when $E_1 \gg m_\mu$ and $E_2 \gg m_\mu$,

5) We made the calculations only for the neutrino component of the neutrino beam (focused positive mesons). Similar calculations should be done for the antineutrino admixture due to wrong sign mesons and for antineutrino beam (negative mesons focused), where we expect similar results. Also we note that in this semi-analytical approach we neglect angular and radial distributions of mesons and assume the uniform distribution of the meson decay point along the decay tube. The exact account for these effects and their correlations is possible by pure Monte-Carlo simulations and is presented in section 6.

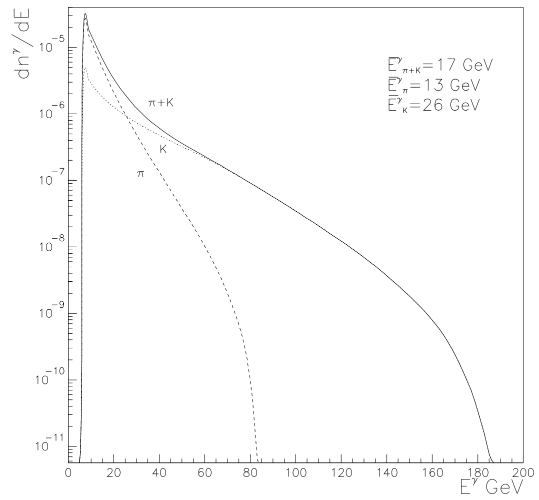

Figure 1: Spectra of muonic photons from internal bremsstrahlung in the CERN 450 GeV neutrino WBB (Wide Band Beam). The muon neutrino mass is assumed to be $m_\nu = 10^{-10}$ eV.

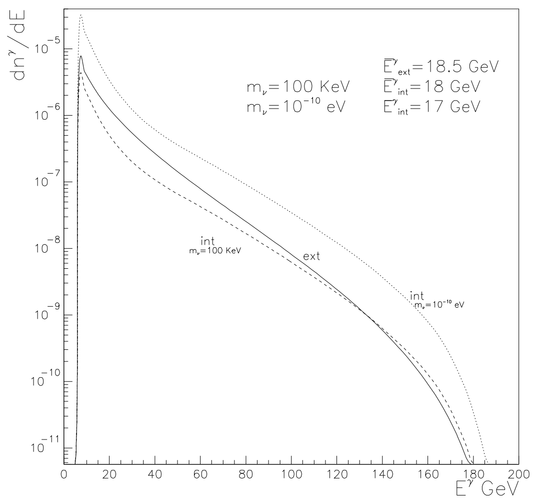

Figure 2: Comparison of the spectrum of muonic photons from internal bremsstrahlung in the CERN 450 GeV WBB neutrino beam for two masses of muon neutrino (dotted line $m_\nu = 10^{-10}$ eV and dashed line $m_\nu = 100$ KeV). The spectrum of muonic photons from external bremsstrahlung is shown by a solid line.

where $E_1(E_2)$ is the energy of the initial (final) muon, we get:

$$d\sigma \;=\; \alpha_\mu \frac{4}{3}\left(\frac{2Z\alpha}{m_\mu}\right)^2 \frac{dE_{\gamma_\mu}}{E_{\gamma_\mu}}\left[1-\frac{E_{\gamma_\mu}}{E_1}+\frac{3}{4}\left(\frac{E_{\gamma_\mu}}{E_1}\right)^2\right]\cdot\left[\ln\frac{2E_1(E_1-E_{\gamma_\mu})}{m_\mu E_{\gamma_\mu}}-\frac{1}{2}-1.5\right]. \qquad (9)$$

Here E_{γ_μ} is muonic photon energy, Z is the charge of a nucleus of iron ($Z = 26$). The term 1.5 appears due to the nuclear form-factor, which was assumed in the form[6)]:

$$F(q^2) = \exp(-q^2a^2/6), \qquad a = (0.58 + 0.82A^{1/3})\mathrm{fm}. \qquad (10)$$

Another parametrization of the nuclear form-factor correction is suggested in ref. [24], according to which, instead of 1.5 in the second bracket of eq. (9), one has to substitute

$$\Delta_n^{el}(\delta) = \ln\frac{D_n}{1+\delta(D_n\sqrt{e}-2)/m_\mu} \quad , \qquad (11)$$

where $D_n = 1.54A^{0.27}$, A - mass number of the nucleus ($A = 56$ for iron), $\delta = m_\mu^2 E_{\gamma_\mu}/2E_1(E_1 - E_{\gamma_\mu})$ – minimal momentum transfer, and $e = 2.718$. The final numerical results of eqs. (9) and (11) are close to each other. In this paper we do not take into account the atomic screening and inelastic form-factors, both nuclear and atomic (see ref. [24]).

The total cross-section of the process (8) convoluted with the spectrum of muons emitted in pion and kaon decays equals to 1760 pb for $\alpha_\mu = 10^{-5}\alpha$. This result was obtained with the help of programs CompHEP and BASES. To calculate the spectrum of muonic photons emitted by muons in the iron shielding we used the formula (9) convoluted with the spectrum of muons. The spectra of muonic photons, produced by the external bremsstrahlung in the iron shielding are presented in fig. 3. The internal and external spectra are compared in fig. 2. First of all, one can see that the yield of muonic photons produced by the internal bremsstrahlung is higher for $m_{\nu_\mu} = 10^{-10}$eV than the yield by the external bremsstrahlung, supporting prospects to measure muonic neutrino mass if γ_μ is discovered. The internal bremsstrahlung spectra are harder than the external ones. Thus increasing the energy of mesons (especially of kaons) should help in measuring neutrino mass. Moreover, the ratio of pion and kaon components is drastically different for muons (and hence for their bremsstrahlung in the shielding) from that for the mesons themselves. Indeed, while initial meson spectrum in the CERN beam has 80.4% decayed

6) An extensive compilation of nuclear elastic form-factors can be found in ref. [28].

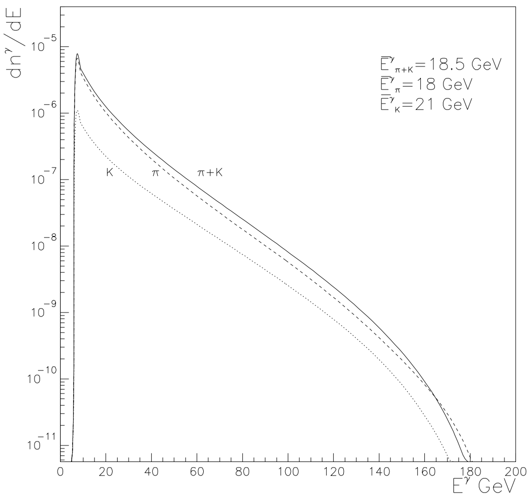

Figure 3: Spectra of muonic photons from external bremsstrahlung in the CERN 450 GeV WBB neutrino beam. The contribution from π-decay is shown as dashed line, from K-decays by dotted line.

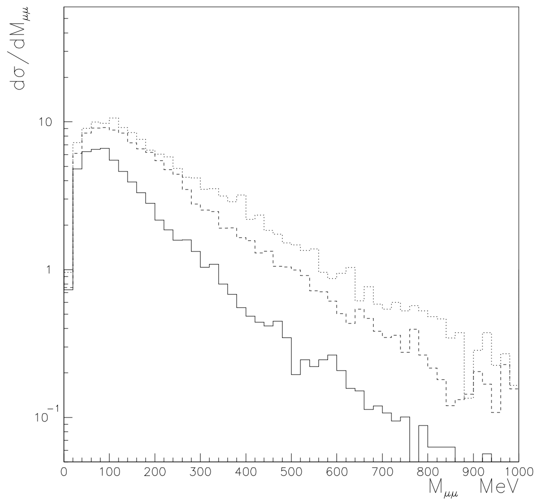

Figure 4: Invariant mass distributions (in units of pb/20 MeV) of muon pair from the conversion in the neutrino detector of muon gammas with fixed energies of 20 GeV (solid), 50 GeV (dashed) and 100 GeV (dotted line).

pions, the muon flux at the end of the decay tunnel has 96.5% muons emitted in the pion decays. The relative enhancement of pion component is caused by a strong suppression of the kaon component, because the muons and muonic gammas from K-decays have wider angular distribution and are partly missing the acceptance of the neutrino detector (see [16] for the corresponding formulas). However the contribution of energetic muons from kaon decays is enhanced by rather high energy cut, 7 GeV, on muonic photons and the increase of the bremsstrahlung cross-section with energy. Finally, 82.9% of muonic photons and 80.3% of muon pairs originate from pions (this effect is discussed in more details in ref. [16]).

In the external bremsstrahlung calculations we have neglected angular distribution of muonic photons in the reaction (8). Indeed, muons, moving at angles larger than the angular size of the detector could, nevertheless, produce muonic photons crossing the detector. Moreover, muons, moving in the directions crossing the detector, could produce muonic photons going outside it. We assume that these two effects more or less compensate each other. The angular distribution of muonic photons produced in the external bremsstrahlung has a forward peak with characteristic polar angle $\theta \sim m_\mu/\bar{E}_1$, where $\bar{E}_1$ is the muon average energy. For $\bar{E}_1 = 31$ GeV , more than 80% of photons lie inside this θ-cone (about $0.2°$). Thus, we assume that the effect under discussion should give a correction factor not larger than 2 in our final results.

4 Photoproduction of muon pairs by γ_μ's.

The photoproduction of muons by ordinary photons has been analysed in a number of papers. The corresponding cross-section is connected with the bremsstrahlung cross-section by crossing (see refs. [19, 20]). One can use the differential cross-section suggested in ref. [29], substituting α_μ instead of α, but keeping the factor $Z\alpha$

$$\begin{aligned} d\sigma(\gamma_\mu + Z \to \mu^+ + \mu^- + Z) &= \alpha_\mu \left(\frac{2Z\alpha}{m_\mu}\right)^2 \left(1 - \frac{4x_+x_-}{3}\right) dx_+ \times \\ &\times \left[\ln\left(\frac{2}{3}\frac{m_\mu}{m_e}\frac{A_0}{Z^{2/3}}\right) - \ln\left(1 + \frac{A_0}{Z^{1/3}}\frac{\delta\sqrt{e}}{m_e}\right)\right]. \end{aligned} \tag{12}$$

Here $\alpha = 1/137$, Z is atomic number of the nucleus ($Z = 10$ for the 'average nucleus' in the CHARM II detector), $\delta = m_\mu^2/2E_{\gamma_\mu}x_+x_-$ – minimal momentum transfer, E_{γ_μ} – the energy of the muonic photon, $x_\pm = E_\pm/E_{\gamma_\mu}$, where $E_\pm$ – energy of $\mu^\pm$, $A_0 \simeq 190$ – a constant, which determines the value of the radiation logarithm.

With $E_{\gamma_\mu} \sim 20$ GeV and $0.1 < x_\pm < 0.9$, the atomic screening may be neglected, so that the logarithmic factor simplifies:

$$\ln\frac{2}{3}\frac{m_\mu}{\delta Z^{1/3}\sqrt{e}} = \ln\frac{4}{3}\frac{E_{\gamma_\mu}x_+x_-}{m_\mu Z^{1/3}} - \frac{1}{2}. \tag{13}$$

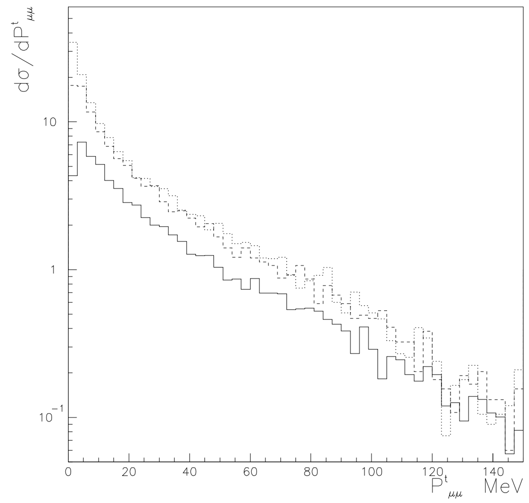

Figure 5: Transverse momentum distributions (in units of pb/3 MeV) of muon pair from the conversion in the neutrino detector of muon gammas with fixed energies of 20 GeV (solid), 50 GeV (dashed) and 100 GeV (dotted line).

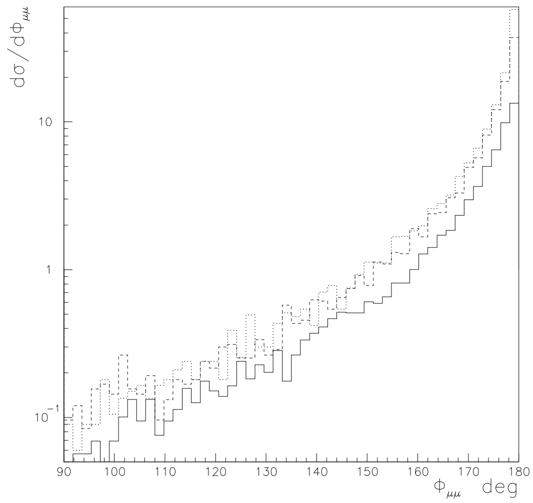

Figure 6: Azimuthal angle distributions (in units of pb/1.8°) between two muons from the conversion in the neutrino detector of muon gammas with fixed energies of 20 GeV (solid), 50 GeV (dashed) and 100 GeV (dotted line).

Another, more recent parametrisation of the same cross section[7)] is:

$$d\sigma = \alpha_\mu \left(\frac{2Z\alpha}{m_\mu}\right)^2 \left(1 - \frac{4x_+x_-}{3}\right) \left[\ln \frac{\frac{B}{Z^{1/3}}\frac{m_\mu}{m_e}}{1 + \frac{B}{Z^{1/3}}\frac{\delta}{m_e}\sqrt{e}} - \ln \frac{D_n}{1 + \frac{\delta}{m_\mu}(D_n\sqrt{e} - 2)}\right] dx_+, \tag{14}$$

where $B = 183,\ D_n = 1.54 \cdot A^{0.27}$ and A is a number of nucleons in a nucleus ($A = 20$ for the 'average nucleus' of the CHARM II detector). Note that for not too small values of the δ parameter ($\delta/m_e \gg Z^{1/3}/B\sqrt{e}$) the square brackets in eq. (14) reminds the last factor of eq. (9) with substitution of the term (-1.5) by eq. (11):

$$\{\} \rightarrow \left[\ln\left(\frac{m_\mu}{\delta}\right) - \frac{1}{2} - \ln \frac{D_n}{1 + \delta(D_n\sqrt{e} - 2)/m_\mu}\right]. \tag{15}$$

Note also that if we neglect both atomic screening and nuclear form-factor and integrate over dx_+, we reproduce an expression similar to the well known result (Ref. [[20]], eq. 32.9)

$$\sigma = \alpha_\mu \frac{7}{9} \left(\frac{2Z\alpha}{m_\mu}\right)^2 \left(\ln \frac{2E_{\gamma_\mu}}{m_\mu} - \frac{109}{42}\right). \tag{16}$$

Similarly to the case of the muon bremsstrahlung in the shielding the nuclear elastic form-factor can be accounted for effectively by introducing an additional term in brackets, -1.2. This value can be obtained from the parametrisation (10) for average nuclei with $Z = 10$, 'neon', in the CHARM II detector. Note that this term equals to -1.5 for Fe ($Z = 26$), see (9).

To get accurate numerical results for cross-section and to calculate distributions for dimuon photoproduction we used the programs CompHEP and BASES/SPRING . In particular, the total cross-section of dimuon photoproduction by an "average" muonic photon, for $\alpha_\mu = 10^{-5}\alpha$, is 41.5 pb in the case of convolution with the normalized spectrum of muonic photons produced by the external bremsstrahlung, and 35.6 pb in the case of the internal bremsstrahlung (with $m_{\nu_\mu} = 10^{-10}$ eV). Note that in the case of internal bremsstrahlung the shapes of all distributions depend only slightly on the neutrino mass. Of course this is caused by the similarity of muonic photon spectra for different neutrino masses (see fig. 2). This similarity can be easily understood as the main contribution comes from the logarithmic terms like that in eq. (6).

Returning to the formula (16) we note that its modified version, with additional term -1.2 effectively accounting for elastic nuclear form-factor, differs from the accurate calculation by CompHEP and BASES by less

[7)] S.R.Kelner, R.P.Kokoulin, private communication

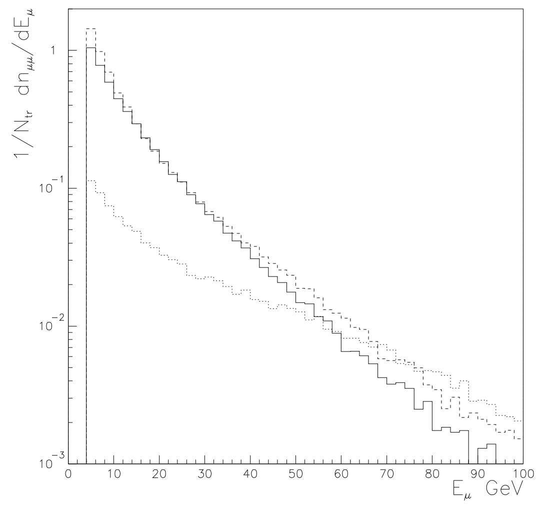

Figure 7: Energy spectra of muons from the conversion of muonic photons and from tridents in the neutrino detector at CERN neutrino beam. Solid line corresponds to external brems, dashed line to internal brems and dotted line to tridents.

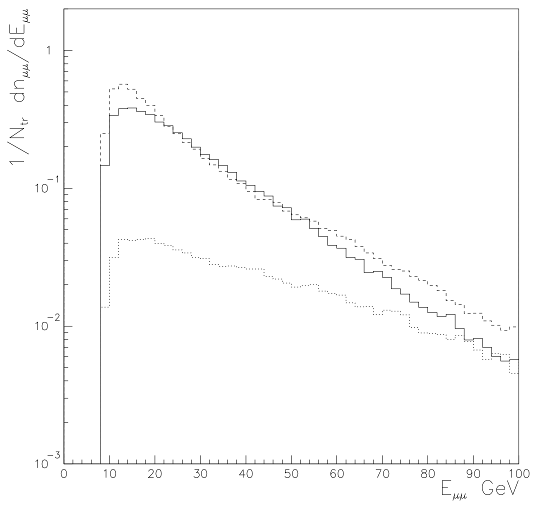

Figure 8: Energy spectra of muon pairs from the conversion of muonic photons and from tridents in the neutrino detector at CERN neutrino beam. Solid line corresponds to external brems, dashed line to internal brems and dotted line to tridents.

than 1% for $E_{\gamma_\mu} > 50$ GeV, and this difference does not exceed 10% for lower energies within the energy range $E_{\gamma_\mu} > 7$ GeV discussed here.

Muons should have high enough energy to be detected; in our calculations we took the detector energy threshold for muons as 4 GeV. Keeping in mind this energy threshold we have applied energy cut 7 GeV on the energies of the original muons and neutrinos and on the energy of muonic photons. However for the final muons, produced in the detector by muonic photons, we have applied cut $E_\mu > 4$ GeV. All values of the photoproduction cross-section given above were obtained with these cuts.

Taking into account the yields of muonic photons, normalized to one muon neutrino from two-body π/K mesons decays, calculated as discussed above (see [16]),

$$\begin{array}{ll} 3.1 \cdot 10^{-7} & \text{ext. brems.,} \\ 1.5 \cdot 10^{-7} & \text{int. brems., } m_{\nu_\mu} = 100 \text{ KeV,} \\ 10.4 \cdot 10^{-7} & \text{int. brems., } m_{\nu_\mu} = 10^{-10} \text{ eV,} \end{array}$$

one can derive the the specific yields of muon pairs per unit neutrino flux:

$$\begin{array}{ll} 2.1 \cdot 10^{-10} & \text{ext. brems. events cm}^2 \text{ /neutrino,} \\ 0.9 \cdot 10^{-10} & \text{int. brems. events cm}^2 \text{ /neutrino , } m_{\nu_\mu} = 100 \text{ KeV,} \\ 5.9 \cdot 10^{-10} & \text{int. brems. events cm}^2 \text{ /neutrino, } m_{\nu_\mu} = 10^{-10} \text{ eV.} \end{array}$$

These specific yields of muon pairs are not exactly proportional to the specific yields of muonic photons because of the difference of the mean energies and effective cross-sections. To obtain these numerical results we took the number of average nuclei (with $Z = 10$, 'neon') in the CHARM II detector equal to $0.16 \cdot 10^{32}$ [10], and $\alpha_\mu = 10^{-5}\alpha$. Neutrino flux in CHARM II experiment is estimated [30] as $8.6 \cdot 10^{11}\ \nu/\mathrm{cm}^2$ integrated over the whole energy spectrum. So we would expect 177 dimuon pairs in CHARM II exposure from muonic photons produced by external bremsstrahlung. Then, in the case of internal bremsstrahlung we should observe about 74 events, if the mass of muonic neutrino is close to the experimental limit, 100 KeV, and more than 511 events, if the mass of muonic neutrino is very small, of order 10^{-10} eV. Invariant mass and transverse momentum of muon pairs, azimuthal angle between two muons distributions are shown on figs. 4, 5, 6 at some fixed energies of muonic photons: 20 GeV (solid lines), 50 GeV (dashed lines) and 100 GeV (dotted lines).

The shapes of the transverse momentum and azimuthal angle distributions scales with energy, while the invariant mass of two muons slightly increases at high energy.

The energy spectra of muons and muon pairs from tridents and from conversion of muonic photons at CERN neutrino WBB are presented in figs. 7 and 8.

In these and following figures we represent external brems by solid lines, internal brems with $m_{\nu_\mu} = 10^{-10}$ eV by dashed lines and tridents by dotted lines. All distributions are normalized to one trident event. One can note

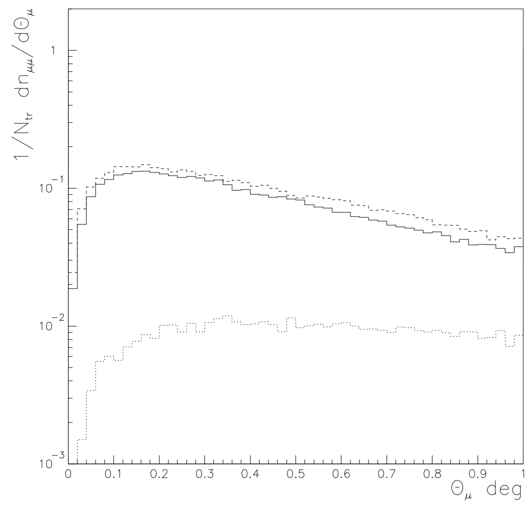

Figure 9: Angular distribution of muons from the conversion of muonic photons and from tridents in the neutrino detector at CERN neutrino beam. Solid line corresponds to external brems, dashed line to internal brems and dotted line to tridents.

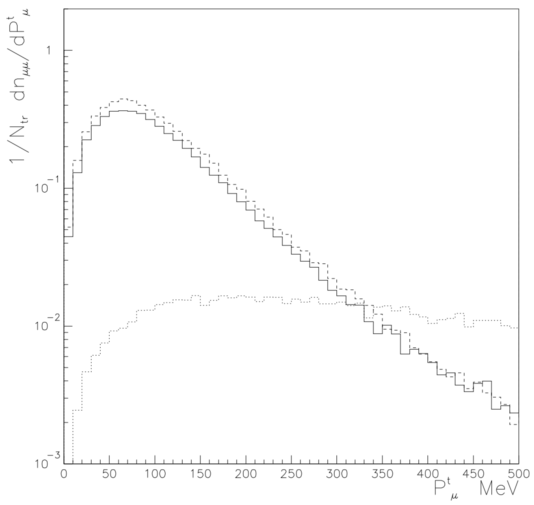

Figure 10: Transverse momentum of muons from the conversion of muonic photons and from tridents in the neutrino detector at CERN neutrino beam. Solid line corresponds to external brems, dashed line to internal brems and dotted line to tridents.

that these spectra are harder in the case of the internal bremsstrahlung than in the external one.

One can see on fig. 9 that muons from γ_μ conversions are produced at small angles: more than 80% at angles less than 1° with respect to the direction of generic muonic photon. We have found also that in both cases (external and internal ones) muons are produced with rather small p_t: 90% of muons have transversal momentum less than 200 MeV (fig. 10).

We also calculated distributions in different kinematical variables to find most effective cuts to localize the effect of muonic photons. In figs. 11, 12, 13, 14 we present the distributions in the invariant mass of dimuons, in the transversal momentum of a muon pair (the so-called p_t-imbalance), in the azimuth angle between muons (it is an angle between the transversal components of μ^+ and μ^- momenta), and in the angle between total momenta of μ^+ and μ^-.

5 The trident background.

As it has been mentioned in the introduction, the main background for the search of muonic pairs produced by muonic photons is presented by tridents, process (5). The cross-section of trident production in a Coulomb field of a nucleus with charge Z, can be easily estimated using Weizsaecker-Williams approximation (see e.g. [31]):

$$\sigma(\nu_\mu + Z \to \nu_\mu + \mu^+ + \mu^- + Z) = \frac{2(Z\alpha)^2 G^2}{9\pi^3}(g_L^2 + g_R^2) \cdot s_{max} \cdot \ln \frac{s_{max}}{4m_\mu^2} \; . \tag{17}$$

Here $G = 1.166 \cdot 10^{-5}\,\mathrm{GeV}^{-2}$ is the four-fermion coupling constant, $g_L = \frac{1}{2} + \sin^2\theta_W$, $g_R = \sin^2\theta_W$, $\sin^2\theta_W = 0.23$, $s_{max} = 2E_1 Q_{max}$, $Q_{max} = 1/a$, where a is the radius of the nucleus, see eq. (10); E_1 is the energy of the initial neutrino. This approximate formula gives the value smaller by $\sim 10\%$ then the accurate calculation using CompHEP and BASES within the discussed energy range. The cross-section convoluted with the normalized neutrino spectrum gives the value $\sigma = 0.045 \cdot 10^{-4}$ pb. This numerical result has been obtained with the nuclear form-factor (10) and with energy cut $E_\mu > 4$ GeV applied on muons. The number of trident events is estimated by using the neutrino flux and target mass given in Section 4 to be 50 events.

Energy spectra of muons, and muon pairs for tridents are presented by dotted lines in figs. 7 and 8. In figs. 11, 12, 14, 13 we present distributions (also by dotted lines) in different variables for tridents — in invariant mass of the muon pair, in transversal momentum of the muon pair (p_t-disbalance), in the angle between muon and antimuon, and in azimuth angle between muon and antimuon. One can see that trident events are distributed in these variables broader than muon pairs in dimuon photoproduction. The characteristic values of kinematical cuts on these variables are collected in table 2, together with the percentage of the background trident events which survive these cuts. It is obvious that the most promising is the cut in the transversal momentum of muon pair,

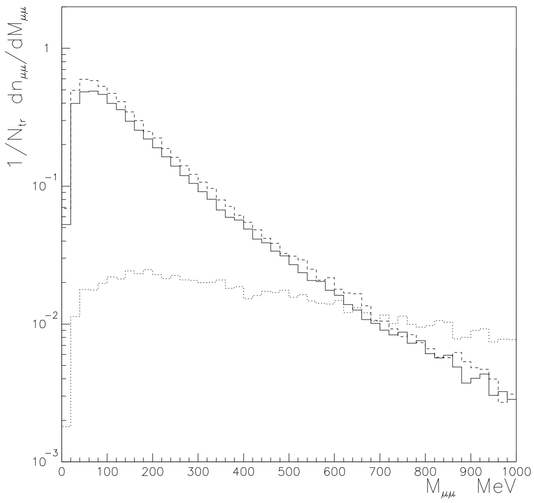

Figure 11: Invariant mass of muons from the conversion of muonic photons and from tridents in the neutrino detector at CERN neutrino beam. Solid line corresponds to external brems, dashed line to internal brems and dotted line to tridents.

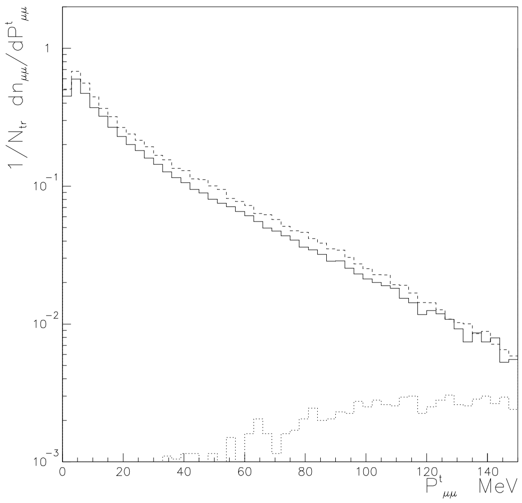

Figure 12: Transverse momentum of muon pair from the conversion of muonic photons and from tridents in the neutrino detector at CERN neutrino beam. Solid line corresponds to external brems, dashed line to internal brems and dotted line to tridents.

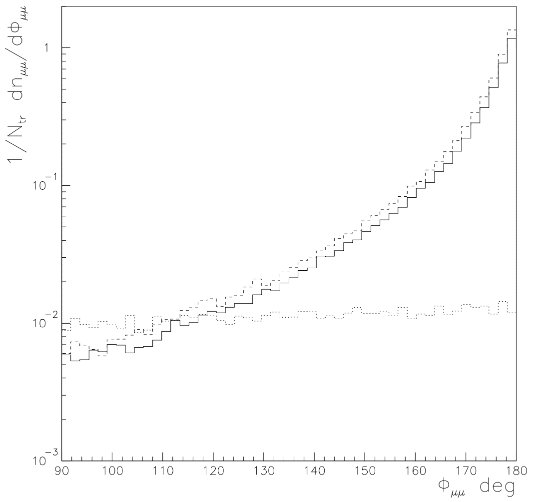

Figure 13: Azimuthal angle between muons from the conversion of muonic photons and from tridents in the neutrino detector at CERN neutrino beam. Solid line corresponds to external brems, dashed line to internal brems and dotted line to tridents.

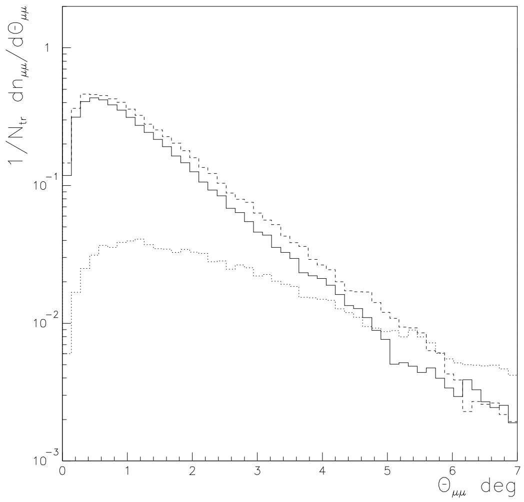

Figure 14: Angle between muons from the conversion of muonic photons and from tridents in the neutrino detector at CERN neutrino beam. Solid line corresponds to external brems, dashed line to internal brems and dotted line to tridents.

Observable	int.brems.	ext.brems.	tridents
$M_{\mu\mu}$(MeV) $<$	500	500	39%
$p_t^{\mu\mu}$(MeV) $<$	72	73	2.12%
p_t^{μ}(MeV) $<$	200	200	24.9%
$\varphi_{\mu\mu}$(deg) $>$	142	142	25.6%
$\vartheta_{\mu\mu}$(deg) $<$	2.8	2.7	64.2%
E_{μ}(GeV) $<$	28	28	65.8%
$E_{\mu\mu}$(GeV) $<$	56	52	69%

Table 2: The kinematical cuts, each of them preserves separately 90% of muon pairs produced by muonic photons in the detector (columns 2 and 3), and the percentage of the trident background events within the cuts given for external bremstrahlung case (column 4). Here $M_{\mu\mu}$ is the invariant mass of a muon pair; p_t^{μ} and $p_t^{\mu\mu}$ are transversal momenta of a muon and a muon pair correspondingly, $\vartheta_{\mu\mu}$ is the angle between μ^+ and μ^-, while $\varphi_{\mu\mu}$ is the angle between their transversal momenta; E_{μ} - energy of a muon (μ^+ or μ^-) and $E_{\mu\mu}$ is energy of a muon pair. For internal bremsstrahlung the numerical results only slightly depend on neutrino mass within the discussed range, at least up to 10^{-10} eV.

p_t-disbalance. Only 2 % of trident events have $p_t^{\mu\mu} < 70$ MeV. By applying this cut one can hope to get the suppression of trident background by a factor 50 while practically all muon pairs from photoproduction will be kept.

The cuts on invariant mass of muon pair and on azimuth angle between two muons could be also effective, each could suppress trident background by a factor 3-4. In addition, we found that distribution in transversal momentum of muons is much broader for tridents than for dimuon photoproduction, here the suppression factor 4 could be also obtained for tridents. Of course special analysis is necessary to find those combinations of these cuts which will give maximal suppression factor for the trident background - the correlations are important.

6 Monte-Carlo simulation of the production and detection of the muonic photons.

In order to take into account the details of the geometry and kinematics of the neutrino beam line, a special CERN Monte-Carlo program was used, which directly simulates the decay of π/K with muonic photon and the bremsstrahlung of muonic photons in the iron shielding of the neutrino beam. This program uses the Monte-Carlo π/K-decays produced by GBEAM program [10] with realistic geometry, magnetic focusing in the horn and reflector and π/K lifetimes. So at the input every event has the coordinates of the π/K decay point and the vector of π/K momentum. The difference with the semi-analytical approach is that the radial and longitudinal spatial distributions of π/K in the decay tunnel, the angular distribution of π/K mesons and their correlations are automatically taken into account. Both positive and negative π/K mesons are used for muonic photon flux calculation in the neutrino Wide Band Beam (WBB), where positive mesons are focused, while negative mesons are defocused.

The internal bremsstrahlung of muonic gammas in π/K decays is generated according to the formulas used in the section 2. The flux of the muonic photons is calculated in the fiducial volume of CHARM-II detector with square cross-section of 3.2x3.2 m^2 located at 882 m from the proton target.

The production of the muonic photons by external bremsstrahlung from muons, stopping in the iron shielding was calculated according to the formula (9). For this study the shielding was approximated by 80 blocks of iron, each 3m in length. The simplified tracking take into account the energy loss of 4.5 GeV per block and multiple scattering of muons in the iron. The muons were tracked down to 10 GeV. Muonic photons were generated with the angular distribution (f.w.h.m. 0.12^o) around the muon direction at each tracking step. The effect of the multiple scattering reduce the flux of muonic photons in the volume of the neutrino detector, because of the increase of the angular spread.

The conversion of muonic photons into muon pairs in the target of the neutrino detector was simulated according to formula (14) for the average CHARM II nuclei (A=20, Z=10). The energy cut of 4 GeV was applied on both muons.

Observable	Semi-analytical	Monte-Carlo
$\overline{E_\gamma^{int}}$	16.8 GeV	17.9 GeV
$\overline{E_\gamma^{ext}}$	18.5 GeV	22.8 GeV
F_γ^{int}/F_ν	$10.4 \cdot 10^{-7}$	$12.5 \cdot 10^{-7}$
F_γ^{ext}/F_ν	$3.1 \cdot 10^{-7}$	$2.3 \cdot 10^{-7}$
σ_γ^{int}	35.6 pb	39.9 pb
σ_γ^{ext}	41.5 pb	53.8 pb
N^{int}	511 events	688 events
N^{ext}	177 events	172 events
$N_{total}^{tridents}$	140 events	138 events
$N_{4\text{GeV}cut}^{tridents}$	49 events	47 events

Table 3: Results of semi-analytical and Monte-Carlo calculations of the following quantities: the average energies of muonic photons ($\overline{E_\gamma^{int}}$, $\overline{E_\gamma^{ext}}$) , the ratios of muonic photon flux to neutrino flux for external F_γ^{int}/F_ν and internal F_γ^{ext}/F_ν bremsstrahlung, the average muonic gamma interaction cross-sections for gammas from internal σ_γ^{int} and external σ_γ^{ext} bremsstrahlung, the numbers of events of muonic gamma conversions from internal N^{int} and external N^{ext} bremstrahlung and the numbers of trident events without ($N_{total}^{tridents}$) and with ($N_{4\text{GeV}cut}^{tridents}$) the cut on muon momentum of 4 GeV. The fluxes, cross-sections and mean energies were calculated with the cut $E_\gamma > 7$ GeV and $E_\mu > 4$ GeV.

The cross-section and rates of the trident background were calculated by Monte-Carlo program [30] with neutrino spectra predicted by GBEAM [10] program. Only coherent part of the cross-section was estimated for this study.

The results of these calculations in the form of the mean energies, cross-sections and rates are summarised in the table 3 for the neutrino mass $m_{\nu_\mu} = 10^{-10}$ eV and $\alpha_\mu/\alpha = 10^{-5}$. The numerical results of this Monte-Carlo simulation are close to the semi-analytical calculations. The differences are due to different approximations and assumptions on the geometry, the spectra of mesons, the effects of multiple scattering and the angular distributions.

7 Measurement of the muon neutrino mass

The measurement of the neutrino mass is the possibility *in principal*, not a proposal for current experiments, as it can be done only in the lucky case of the observation of the strong signal of muonic gamma. There are several ways of doing it. For example there is an elegant gedanken experiment:

- 1. First one measures the rate of the muonic gammas in the classical neutrino beam. Then the experimental rate is:

$$N_{exp1} = N_{intbrems}(\alpha_\mu, m_{\nu_\mu}) + N_{extbrems}(\alpha_\mu)$$

Note that external bremsstrahlung rate does not depend on m_{ν_μ}.

- 2. Second one installs strong magnets at the end of the decay tunnel to sweep out most of the muons from the direction of the detector. In this case:

$$N_{exp2} = N_{intbrems}(\alpha_\mu, m_{\nu_\mu})$$

Solving these two equations one will get:

$$N_{extbrems}(\alpha_\mu) = N_{exp1} - N_{exp2}$$

From this equation one determines the coupling constant α_μ. Plugging this coupling constant into first equation one gets the estimate of m_{ν_μ}. Certainly one needs good statistics, otherwise the precision of the mass measurement would be poor due to small logarithmic slope of the function. One can also try to use the difference in the energy spectra of internal and external gammas. Another approach would be to measure the coupling independently, if the g-2 experiment is improved by an order of magnitude in its accuracy and shows discrepancy with QED.

8 Supernovae

In recent paper S.N.Gninenko [32] remarked that muonic photons should be produced in the cores of supernovas. This may modify the dynamics of collapse due to an additional cooling of the supernovas. The legimite question is if this excludes the range of the coupling constants under consideration in the present paper. According to Gninenko the upper limit on α_l from SN 1987A is 1.6×10^{-11}. However he noted that for values larger than

1.6×10^{-7} the leptonic photons "become trapped and no longer contribute effectively to the SN1987A luminosity". So his conclusions is: "Since this estimate gives only a correct order of magnitude for the lower limit on α_l, we believe that the region of $\alpha_l = O(10^{-7})$ might still be of interest for searching for leptonic photons in neutrino experiments." [8] However Gninenko does not take into account the reaction $\gamma_l \mu \to \gamma\mu$, which has the cross-section larger at least by a factor 10^5 than those of elastic $\gamma_l \nu$-scattering, that he used in the calculation of the mean free path of the leptonic photons. If he would taken this into account the leptonic photons with $\alpha_l > 0.7 \cdot 10^{-10}$ would be trapped in the core. In this case there is no astrophysical limitations in the range of sensitivity of accelerator experiments. The importance of the μ content in the supernovae core was pointed out by G.V.Domogatsky [33] and discussed by S.I.Blinnikov [34]. In any case the accelerator experiment would be complementary to the astrophysics limit.

Conclusions.

Let us summarize the main results of this paper. If $\alpha_\mu \sim 10^{-5}\alpha$, as allowed by $(g-2)_\mu$ data, then in the high-energy neutrino experiment of the type of CHARM II one may observe ~ 180 narrow muon pairs produced by muonic photons in the case of external bremsstrahlung. In the case of internal bremsstrahlung there may observe about 70 events if the mass of muonic neutrino is 100 KeV, and ~ 600 events if the mass of muonic neutrino is very small, of order 10^{-10} eV. This should be compared with approximately 50 muon pairs from trident events. Thus, muonic photons could be discovered in such experiments if $\alpha_\mu \sim 10^{-5}\alpha$. Moreover, one may hope to measure the mass of muonic neutrino if this mass is small enough and muonic photon is discovered.

By selecting pairs with $p_t < 70$ MeV one may reduce the number of background trident pairs by a factor of 50, to a few events. One may hope to further suppress the trident background by selecting muon pairs with invariant mass less than 500 MeV, or with azimuth angle between muons larger than $140°$, or with transversal momentum of muon and antimuon smaller than 200 MeV. Thus, if no events satisfying the cuts are observed, one can reach the sensitivity of $\alpha_\mu/\alpha < 10^{-6}$.

Acknowledgements

The authors are grateful to K. Winter whose questions about the difference between the muon pairs from muonic photons and tridents initiated this work. L.O. is grateful to R.R. Kokoulin, S.R. Kelner, S.A. Maltsev, A.Yu. Morozov, L.I. Rozental, A.V. Smilga, M.J. Tannenbaum, V.R. Zoller for interesting discussions, and to RFBR for the grants 96-02-18010 and 96-15-96578. V.I. is grateful to E.E. Boos and A.E. Pukhov for useful discussions, and to the European association INTAS (contract 93-1180ext) and the Grant Center for Natural Sciences of State Committee for Higher Education in Russia (grant 95-0-6.4-38). A.R. is grateful to CHARM-II/CHORUS and CPPM colleagues for interesting discussions and support.

[8] At this section we use notation $\gamma_l(\alpha_l)$ instead of $\gamma_\mu(\alpha_\mu)$.

References

[1] E. Eskut et al.,CHORUS Collaboration. Nucl.Instr.Methods **A401** (1997) 7.

[2] J. Altegoer et al. NOMAD Collaboration. Preprint CERN-PPE-97-059. Subm. to Nucl. Instrum. Methods (1997).

[3] T.D. Lee and C.N. Yang. Phys.Rev. **98** (1955) 1501.

[4] L.B. Okun. Yadernaya Fizika **10** (1969) 359 (in Russian); Sov. Journal of Nucl.Phys. **10** (1969) 206.

[5] L.B. Okun, Phys.Lett. **B382** (1996) 389-392;

[6] L.B. Okun. 'Leptons and Quarks'. North Holland. 1984. Chapter 19, p. 166.

[7] A.K. Ciftci, S. Sultansoi, and S. Türköz. Phys. Lett. **B355** (1995) 494.

[8] S.I. Blinnikov, A.D. Dolgov, L.B. Okun, and M.B. Voloshin. Nucl. Phys. **B458** (1996) 5264.
L.B. Okun, 'A remark on leptonic photons'. June 1972 (Unpublished manuscript in Russian, presented at the ITEP theoretical seminar).

[9] L.B. Okun, Mod. Phys. Lett. **A11** (1996) 3041.

[10] C.Foos et al., GBEAM - neutrino beam simulation program, CHARM II Internal Note, Nov 1989.

[11] Review of Particle Properties. Phys. Rev. **D54**, No. 1 (1996), Part 1.

[12] E.E. Boos, M.N. Dubinin, V.A. Ilyin, A.E. Pukhov, and V.I. Savrin. 'CompHEP – specialised package for automatic calculation of elementary particle decays and collisions'. Preprints SNUTP 94-116, Seoul, 1994; INP MSU 94-36/358; hep-ph/9503280.

[13] V.A. Ilyin, D.N. Kovalenko and A.E. Pukhov, I.J.Mod.Phys.,**C7** (1996) 761.

[14] S. Kawabata. Comp. Phys. Commun. **41** (1986) 127.

[15] A.C. Hearn and J.Fitch, 'REDUCE USER'S MANUAL', version 3.6. The Rand Publication, CP87 (Rev. 7/95), 1995.

[16] V.A.Ilyin, Note on the method of muon, neutrino and muon gamma spectra calculation with geometrical and angular acceptance (1997).

[17] H.A. Bethe and W. Heitler. Proc. Roy. Soc. London **A146** (1934) 83.

[18] H.A. Bethe. Proc. Cambr. Phil. Soc. **30** (1934) 524.

[19] W. Heitler. 'The Quantum Theory of Radiation'. Thirds edition, Oxford, Clarendou Press, 1954, §25.

[20] A.I. Akhiezer and V.B. Berestetsky. 'Kvantovaya Electrodinamika'. Third edition, Nauka Publishers, Moscow 1969, §28. (in Russian)
'Quantum Electrodynamics', §29, Interscience Publisher, New York, 1965.

[21] A.A. Petrukhin and V.V. Shestakov, Can. J. Phys. **46** (1968) §377.

[22] I.L. Rozental. Uspekhi Fiz. Nauk **94** (1968) 91 (in Russian); Sov. Phys. Uspekhi **11** (1968) 49.

[23] R.P. Kokoulin and A.A. Petrukhin. In: Proceedings of the International Conference on Cosmic Rays (Hobart, Australia, August 1971), vol. 4, p. 2436.

[24] S.R. Kelner, R.P. Kokoulin and A.A. Petrukhin. 'About cross-section for high-energy muon bremsstrahlung'. Preprint 024-95, Moscow State Engineering Physics Institute. Moscow 1995.

[25] Yu.M. Andreev, L.B. Bezrukov and E.V. Bugaev. Yadernaya Fizika **57** (1994) 2146 (in Russian); Phys. of Atomic Nuclei **57** (1994) 2066.

[26] M.J. Tannenbaum. CERN-PPE/91-134 (1991) (unpublished).

[27] See [11] , p. 137.

[28] H. de Vries, C.W. de Jager, and C. de Vries. 'Nuclear Charge-density-distribution parameters from elastic electron scattering'. In: 'Atomic Data and Nuclear Data Tables', **36** (1987) 495.

[29] R.P. Kokoulin and A.A. Petrukhin. In: 'Kosmofizika', ed. V.V. Dmitrienko, Energoatomizdat, Moscow, 1987, p. 76 (in Russian).

[30] CHARM II Collaboration, A new measurement of the cross-section for trilepton production induced by muon neutrinos (in preparation).

[31] See [6], Chapter 16, p. 140. Corrected in the second Russian edition: 'Leptony i kvarki', Moskva, Nauka, 1990, p.158.

[32] S.N. Gninenko,HEP-PH/9708465, preprint INR-0951; Phys.Lett. **B413** (1997) 365.

[33] G.V. Domogatsky, Nauchnnye Informacii Astronomical Council Ac.Sci.USSR **13** (1969) p.94.
G.V. Domogatsky, preprint INR-96,(1973).

[34] S.I. Blinnikov, Comments on number of muon pairs in collapsing supernovae, (in preparation).